+



Magnetic properties of $L1_0$ FePt thin film influenced by recoverable strains stemmed from the polarization of $Pb(Mg_{1/3}Nb_{2/3})O_3$-$PbTiO_3$ substrate

Li-Wang Liu(刘立旺), Cheng-Chao Hu(胡成超), Ye-Chuan Xu(徐野川), Hou-Bing Huang(黄厚兵), Jiang-Wei Cao(曹江伟), Linyun Liang(梁林云), Wei-Feng Rao(饶伟锋)

Citation: Chin. Phys. B . 2018, 27(7): 077503. **doi:** 10.1088/1674-1056/27/7/077503

Journal homepage: http://cpb.iphy.ac.cn; http://iopscience.iop.org/cpb

What follows is a list of articles you may be interested in

Strong anti-strain capacity of CoFeB/MgO interface on electronic structure and state coupling

Fei Guo(郭飞), Yaping Wu(吴雅苹), Zhiming Wu(吴志明), Ting Chen(陈婷), Heng Li(李恒), Chunmiao Zhang(张纯淼), Mingming Fu(付明明), Yihong Lu(卢奕宏), Junyong Kang(康俊勇)

Chin. Phys. B . 2018, 27(1): 017502. **doi:** 10.1088/1674-1056/27/1/017502

FePt nano-stripes fabricated on anodic aluminum oxide templates

Deng Chen-Hua, Qiao Xin-Yu, Wang Fang, Fan Jiu-Ping, Zeng Hao, Xu Xiao-Hong

Chin. Phys. B . 2015, 24(7): 077504. **doi:** 10.1088/1674-1056/24/7/077504

Tuning the magnetic anisotropy of CoFeB grown on flexible substrates

Zhang Hao, Li Yuan-Yuan, Yang Mei-Yin, Zhang Bao, Yang Guang, Wang Shou-Guo, Wang Kai-You

Chin. Phys. B . 2015, 24(7): 077501. **doi:** 10.1088/1674-1056/24/7/077501

$L1_0$ FePt thin films with [001] crystalline growth fabricated by ZnO addition and rapid thermal annealing

Liu Xi, Ishio Shunji

Chin. Phys. B . 2013, 22(8): 087504. **doi:** 10.1088/1674-1056/22/8/087504

Composition influence on the microstructures and magnetic properties of FePt thin films

Liu Li-Wang, Dang Hong-Gang, Sheng Wei, Wang Ying, Cao Jiang-Wei, Bai Jian-Min, Wei FuLin

Chin. Phys. B . 2013, 22(4): 047503. **doi:** 10.1088/1674-1056/22/4/047503

Magnetic properties of $L1_0$ FePt thin film influenced by recoverable strains stemmed from the polarization of $Pb(Mg_{1/3}Nb_{2/3})O_3$–$PbTiO_3$ substrate*

Li-Wang Liu(刘立旺)[1], Cheng-Chao Hu(胡成超)[2], Ye-Chuan Xu(徐野川)[1], Hou-Bing Huang(黄厚兵)[3], Jiang-Wei Cao(曹江伟)[4], Linyun Liang(梁林云)[5], and Wei-Feng Rao(饶伟锋)[1,†]

[1] *Department of Materials Physics, and IEMM, Nanjing University of Information Science and Technology, Nanjing* 210044, *China*
[2] *College of Materials Science and Engineering, Liaocheng University, Liaocheng* 252059, *China*
[3] *Department of Physics, University of Science and Technology Beijing, Beijing* 100083, *China*
[4] *Key Laboratory for Magnetism and Magnetic Materials of the Ministry of Education, Lanzhou University, Lanzhou* 730000, *China*
[5] *Mathematics and Computer Science Division, Argonne National Laboratory, Argonne, Illinois* 60439, *USA*

(Received 30 December 2017; revised manuscript received 25 April 2018; published online 25 June 2018)

The magnetic properties and magnetization reversible processes of $L1_0$ FePt (3 nm)/$Pb(Mg_{1/3}Nb_{2/3})O_3$–$PbTiO_3$ (PMN–PT) heterostructure were investigated by using the phase field model. The simulation results show that the magnetic coercivities and magnetic domains evolution in the $L1_0$ FePt thin film are significantly influenced by the compressive strains stemming from the polarization of single crystal PMN–PT substrate under an applied electric field. It is found that the magnetic coercivities increase with increasing of the compressive strain. A large compressive strain is beneficial to aligning the magnetic moments along the out-of-plane direction and to the enhancement of perpendicular magnetic anisotropy. The variations of magnetic energy densities show that when compressive strains are different at the magnetization reversible processes, the magnetic anisotropy energies and the magnetic exchange energies firstly increase and then decrease, the negative demagnetization energy peaks appear at coercivities fields, and the magnetoelastic energies are invariable at large external magnetic field with the energy maximum appearing at coercivities fields. The variations of the magnetoelastic energies bring about the perpendicular magnetic anisotropy so that the magnetoelastic energy is lower at the large external magnetic fields, whereas the appearance of magnetoelastic energy peaks is due to the magnetization-altered direction from the normal direction of the plane of the $L1_0$ FePt thin film at coercivities fields.

Keywords: FePt, strain, magnetoelastic energy, phase field

PACS: 75.50.Ss, 75.70.–i, 75.78.Cd, 77.80.bn **DOI:** 10.1088/1674-1056/27/7/077503

1. Introduction

$L1_0$ FePt nanostructures have been extensively studied in many magnetic and magnetoelectric devices, such as late-model heat assisted magnetic recording media,[1–3] permanent magnets,[3–5] and magnetic heterostructures,[6–13] due to their large perpendicular magnetic anisotropy (PMA), excellent chemical stability, and good corrosion resistance.[14–19] The dependence of PMA on the structural domain orientation is vital to the performance of aforementioned applications. Ordered $L1_0$ FePt thin films include three different orientations of the structural domains, one of which is out-of-plane ordered structural domains (OPOSDs) and the other two are in-plane ordered structural domains (IPOSDs). In general, the OPOSDs are desired in microminiature devices.[20] However, not all of the structural domains are OPOSDs in the fabricated $L1_0$ FePt thin films. In order to fabricate high-quality $L1_0$ FePt thin films, many research groups conducted experimental studies on obtaining the designed OPOSDs by changing temperature, deposition pressure, segregants, deposition technique,[21] substrates,[2,22] and so on. Among these, the misfit strain between the thin films and substrate can have a large effect on the formation of the OPOSDs in $L1_0$ FePt thin films based on the experimental measurements. Wang *et al.*[2] and Ho *et al.*[20] measured the effect of misfit strains between the $L1_0$ FePt thin films and substrate on the orientations of structural domains by using a transmission electron microscope (TEM) based automated orientation imaging microscopy technique. The maximal volume of the OPOSDs can only reach 76%,[2,20] and the rest of the structural domains that result in the in-plane magnetic anisotropy need to be reduced in order to improve the PMA in the $L1_0$ FePt thin films. One of the important factors to reduce the volume of IPOSDs is to change the strain states between the $L1_0$ FePt thin films and substrate. Many experimental results[1,20,22] showed that the large lattice mismatch between the $L1_0$ FePt thin films and substrates can cause tensile stress to the $L1_0$ FePt thin films, resulting in a large volume of OPOSDs and a large PMA.

Nevertheless, one experimental work[23] showed that the

*Project supported by the National Natural Science Foundation of China (Grant Nos. 11474167, 51701091, and 11504020) and the Start-up Funds of NUIST, China (Grant Nos. 2243141601035 and 2243141601018).

†Corresponding author. E-mail: wfrao@nuist.edu.cn

© 2018 Chinese Physical Society and IOP Publishing Ltd

value of coercivities increased with the increase of the recoverable compressive misfit strain in the $L1_0$ FePt (3 nm) thin film deposited on PMN–PT substrate. The reason is that when the PMN–PT substrate is polarized under an applied electric field, a recoverable strain is induced by a converse piezoelectric effect, which can pass on to the $L1_0$ FePt thin film and thus manipulate the magnetic anisotropy of the film through the converse magnetostriction effect. Their results[23] also showed that when the electric field increased to ± 10 kV/cm, the value of the recoverable compressive strain can reach at least to -0.06%. However, there are few studies on how the misfit strain variations affect the formation and volume of OPOSDs in $L1_0$ FePt thin films, especially on the mechanism of magnetic domain evolution, which rely on ordered structural domains influenced by strain variations in the ultrathin $L1_0$ FePt thin films.[24] Accordingly, it is essential to investigate the mechanisms of the magnetic domain evolutions and magnetic properties in the $L1_0$ FePt thin films under misfit strains for future applications. To this end, we apply the phase field simulation approach to study the effect of the recoverable strain on the magnetic properties in the $L1_0$ FePt thin film.

The phase field method is a powerful tool to simulate the magnetic domain structure evolution and the resultant properties in various magnetic materials,[25–32] which provides useful guidelines for a precise engineering of magnetic domain structures in magnetic thin films.[33,35] Although the $L1_0$ FePt thin films are usually polycrystalline or doped for practical applications, a basic study on the single crystal $L1_0$ FePt thin film deposited on single crystalline PMN–PT substrates can give a better understanding to the physical mechanisms of the strain-induced magnetic domain structure and properties.

In this work, in the light of the experimental work reported in Ref. [23], the effect of the recoverable compressive strains on the PMA, magnetic domains evolution, and out-of-plane magnetic moments components in the single crystal $L1_0$ FePt (3 nm) thin film were studied in detail by using the three-dimensional phase field model based on Khachaturyan's microelastic theory.

2. Phase field method

The vector magnetization $\boldsymbol{M}$ is chosen as the phase field variable to describe the magnetic domain structures in the $L1_0$ FePt thin film. The spatial and temporal evolutions of $\boldsymbol{M}$ are controlled by the Landau–Lifshitz–Gilbert (LLG) equation[33–35]

$$\frac{\partial \boldsymbol{M}}{\partial t} = -\frac{\gamma_0}{(1+\alpha^2)}\boldsymbol{M}\times\boldsymbol{H}_{\text{eff}} - \frac{\gamma_0\alpha}{(1+\alpha^2)M_{\text{s}}}\boldsymbol{M}\times(\boldsymbol{M}\times\boldsymbol{H}_{\text{eff}}), \quad (1)$$

where γ_0 is the gyromagnetic ratio and α is the damping constant, with a value of 2.211×10^5 $\text{A}^{-1}\cdot\text{s}^{-1}$ and 0.1 in this simulation, respectively. $\boldsymbol{M} = M_{\text{s}}\boldsymbol{m} = M_{\text{s}}(\boldsymbol{m}_1, \boldsymbol{m}_2, \boldsymbol{m}_3)$, in which M_{s} is the saturation magnetization, and $\boldsymbol{m}_i$ is the direction cosine. $\boldsymbol{H}_{\text{eff}}$ is the effective magnetic field, and $\boldsymbol{H}_{\text{eff}} = -\mu_0 M_{\text{s}}\delta E_{\text{total}}/\delta\boldsymbol{M}$, namely, $(\boldsymbol{H}^1_{\text{eff}}, \boldsymbol{H}^2_{\text{eff}}, \boldsymbol{H}^3_{\text{eff}}) = -\mu_0 M_{\text{s}}(\delta E_{\text{total}}/\delta\boldsymbol{M}_1, \delta E_{\text{total}}/\delta\boldsymbol{M}_2, \delta E_{\text{total}}/\delta\boldsymbol{M}_3)$. Also, E_{total} is the total magnetic free energy of the $L1_0$ FePt thin film, which is constructed as

$$E_{\text{total}} = \int [E_{\text{anis}} + E_{\text{stat}} + E_{\text{exch}} + E_{\text{elas}} + E_{\text{exte}}]\,\text{d}V, \quad (2)$$

where E_{anis}, E_{stat}, E_{exch}, E_{elas}, and E_{exte} are the magnetocrystalline anisotropy energy, magnetostatic energy, exchange energy, magnetoelastic energy, and Zeeman energy, respectively. The magnetoelastic energy E_{elas} is given as[33–36]

$$\begin{aligned} E_{\text{elas}} &= \frac{1}{2}\int C_{ijkl}\varepsilon^{\text{elas}}_{ij}\varepsilon^{\text{elas}}_{kl}\,\text{d}V \\ &= \frac{1}{2}\int C_{ijkl}(\varepsilon^{\text{total}}_{ij} - \varepsilon^{\text{eign}}_{ij})(\varepsilon^{\text{total}}_{kl} - \varepsilon^{\text{eign}}_{kl})\,\text{d}V, \end{aligned} \quad (3)$$

where C_{ijkl} are the elastic coefficients, $\varepsilon^{\text{elas}}_{ij}$ is the elastic strain, and $\varepsilon^{\text{total}}_{ij}$ is the total strain, while $\varepsilon^{\text{eign}}_{ij}$ is the eigenstrain related to the local magnetization and given by[31–33]

$$\varepsilon^{\text{eign}}_{ij} = \begin{cases} \dfrac{3}{2}\lambda_{100}\left(m_i m_j - \dfrac{1}{3}\right), & (i=j), \\ \dfrac{3}{2}\lambda_{111} m_i m_j, & (i\neq j), \end{cases} \quad (4)$$

where λ_{100} and λ_{111} are the magnetostrictive coefficients.

The magnetoelastic energy is obtained through combining Khachaturyan's elastic theory and constraint boundary conditions as reported in Refs. [36] and [37]. The temporal evolution of the local magnetization is obtained by solving the Landau–Lifshitz–Gilbert (LLG) equation. The size of $L1_0$ FePt thin film is 256 nm $\times$ 256 nm $\times$ 3 nm. The time step for integration is 2.4×10^{-13} s. The following parameters were used in the simulation in consistence with the experimental work:[23] the saturation magnetization M_{s} of the $L1_0$ FePt thin film is 1140 emu/cc, the magnetic anisotropic constant K_{u} is taken as 1.64×10^5 erg/cc, the exchange constant A_{ex} is 1.0×10^{-10} J/m, the demagnetization factor N_z in the z direction is 1.0, the magnetostriction coefficient λ_{100} is 70×10^{-6}, λ_{111} is 0, and the elastic coefficient C_{11}, C_{12}, and C_{44} are 304 GPa, 223 GPa, and 107 GPa, respectively.

3. Results and discussion

The shape of magnetic hysteresis loops and magnetic coercivities of the $L1_0$ FePt thin films play an important role in determining the properties of magnetoelectrical microminiature devices. Figure 1 shows the effect of compressive strain on the magnetic hysteresis loops and magnetic coercivities of the $L1_0$ FePt (3 nm) thin film. To compare the magnetic coercivities calculated by the phase field method with

the magnetic coercivities measured by the anomalous Hall effect experimental method as reported in Ref. [23], area D in the magnetic hysteresis of the $L1_0$ FePt (3 nm) thin film in Fig. 1(a) is enlarged in Fig. 1(b), which shows that the magnetic coercivity is 2.885 kOe when the strain is 0. The simulated coercivity agrees well with the reported experimental value of 2.88 kOe.[23] The magnetic coercivity gradually increases with decreasing strain from 0 to −0.06% and reaches to 3.178 kOe when the strain is −0.06%. The increase of magnetic coercivities can be attributed to the contribution of the magnetoelatic energy to the magnetic anisotropy energy and will be explained later in the energy density analysis after afterwards. Table 1 shows the comparison between the experimental[23] and calculated coercivities. It can be seen that the simulated coercivities are consistent with experimental results. The minor differences might have originated from the inhomogeneous microstructure of the fabricated $L1_0$ FePt thin film. It is worth mentioning that the magnetic coercivities calculated by the phase field method decrease with the increasing tensile strains. Thus the magnetic properties of the $L1_0$ FePt thin films can be effectively regulated by using tensile or compressive strains.

Table 1. Comparison of the magnetic coercivities of the $L1_0$ FePt (3 nm) thin film between the experimental[23] and the simulation results.

Strain/%	0.00	–0.02	–0.03	–0.04	–0.05	–0.06
Experimental coercivities/kOe	2.880	2.983	3.076	3.105	3.127	3.145
Simulated coercivities/kOe	2.885	2.988	3.037	3.085	3.130	3.178

Figure 2 shows the magnetic domain structures corresponding to the points A, B, C, D, E, and F in the simulated hysteresis loops of the $L1_0$ FePt (3 nm) thin film with the strain of −0.06% in Fig. 1(a). In each of the figures of the magnetic domain structures, the upper part is the plane-view image and the bottom part is the cross-section image of the magnetic domain structures in $L1_0$ FePt thin film and PMN–PT substrate. Figure 2(a) shows that the magnetization is perpendicular to the in-plane direction of the $L1_0$ FePt thin film. When the switching magnetic field is −1.5 kOe (point B), the magnetization reverses from the [001] direction and forms the [101], $[\bar{1}01]$, $[0\bar{1}1]$, and [011] magnetic domains, as shown in Fig. 2(b). Figure 2(c) displays that 50.6% of the statistical [001] magnetic domain volume has deviated from [001] direction, while, [101], $[\bar{1}01]$, $[0\bar{1}1]$, and [011] magnetic domain structures are increasing, and [111], $[\bar{1}11]$, $[11\bar{1}]$, and $[1\bar{1}\bar{1}]$ magnetic domain structures are forming with the switch magnetic field increased to −2.0 kOe (point C). It can be seen that the magnetization lies in a random state, and the [001] and $[00\bar{1}]$ magnetic domains are merely around 3% of the magnetic domain volume, as presented in Fig. 2(d), when the switch magnetic field reaches the coercivity −3.178 kOe (point D). In Fig. 2(e), the $[00\bar{1}]$ magnetic domain increases when the switch magnetic field increases to −12.0 kOe, and $[01\bar{1}]$, $[0\bar{1}\bar{1}]$ magnetic domains have not finished reversing to the $[00\bar{1}]$ direction. Finally, when the switch magnetic field increases to the saturated field −20 kOe, the magnetization completely reverses to the $[00\bar{1}]$ direction, as indicated in Fig. 2(f).

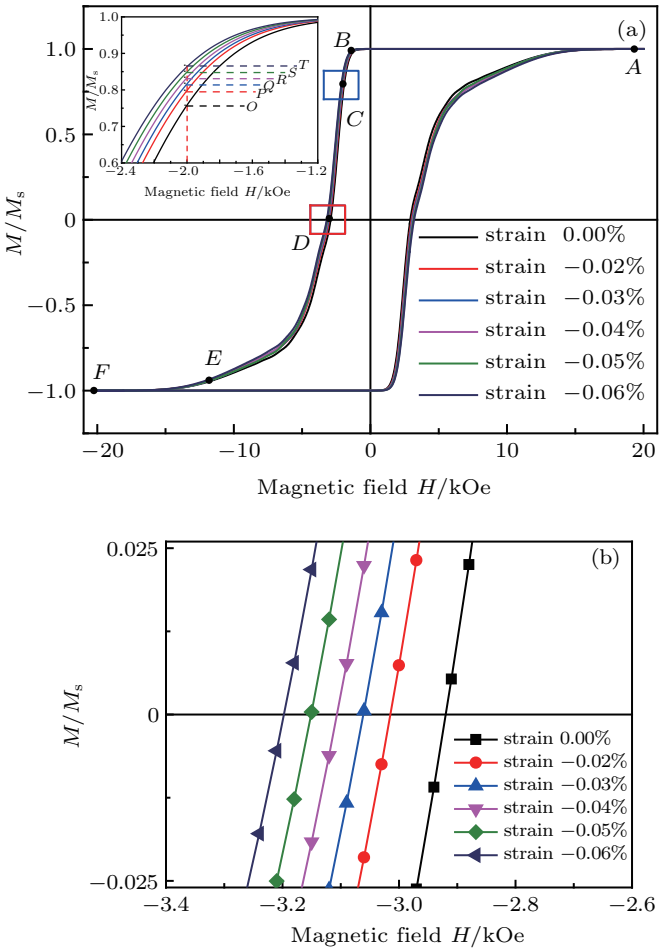


Fig. 1. (color online) (a) Simulated magnetic hysteresis loops and (b) the enlargement of area D in the hysteresis loops of the $L1_0$ FePt (3 nm) thin film with different compressive strains produced by the PMN–PT substrate under the applied electric field.

Figure 3 shows the evolution of simulated magnetic domain structures of the $L1_0$ FePt (3 nm) thin film in different magnetization reversible processes with different compressive strains under the same switch magnetic field $H = 2.0$ kOe (point C). The magnetic domain structures in Figs. 3(a)–3(f) correspond to the point O, P, Q, R, S, and T in inset of Fig. 1(a), respectively. Figure 3(a) shows that the volume fraction of the [001] magnetic domain is 29.3% without any compressive strain, which means 70.7% of the volume fraction of the [001] magnetic domain changes into other orientation magnetic domains. When there is a trivial compressive strain −0.02% acting on the $L1_0$ FePt thin film, the volume fraction of the [001] magnetic domain is 35.1% as displayed in Fig. 3(b). The volume fraction of the [001] magnetic domain increases from 38.6% to 49.4% when the compressive strain

changes from −0.03% to −0.06%, as shown in Figs. 3(c)–3(f). It demonstrates that when the compressive strain becomes larger, the reversal of the magnetization along the [001] direction becomes slower. In other words, it establishes that when the compressive strain increases, the magnetization perpendicular to the $L1_0$ FePt thin film plane inclines to align to the [001] direction and reverses tardily compared to the one without compressive strain. This can be explained by considering the magnetic energy contribution to the $L1_0$ FePt thin film.

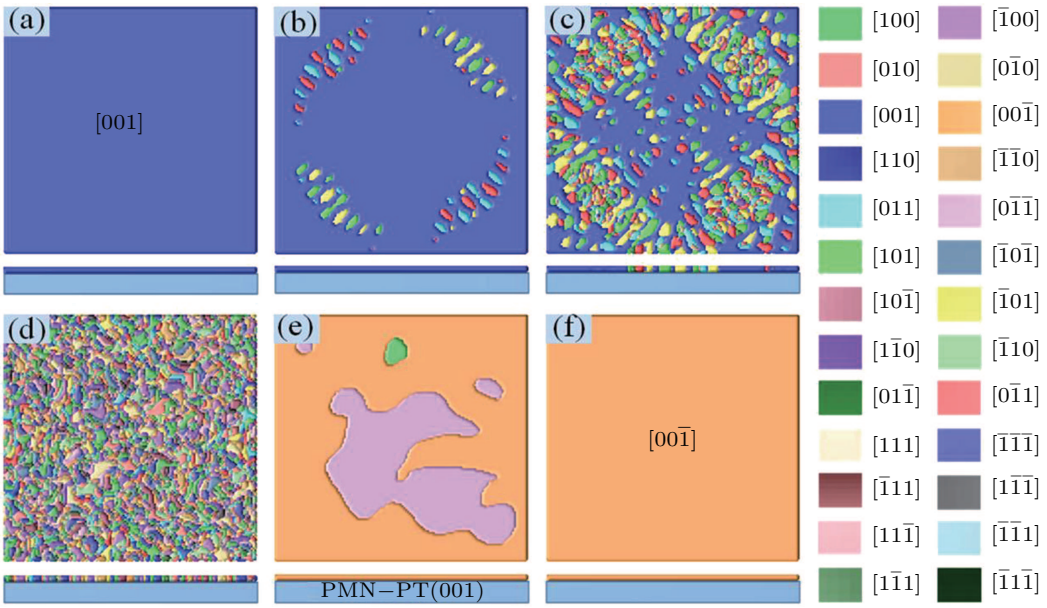


Fig. 2. (color online) Simulated magnetic domain structures, (a)–(f) correspond to the points *A*–*F* in the hysteresis loops of the $L1_0$ FePt (3 nm) thin film when the compressive strain is −0.06%.

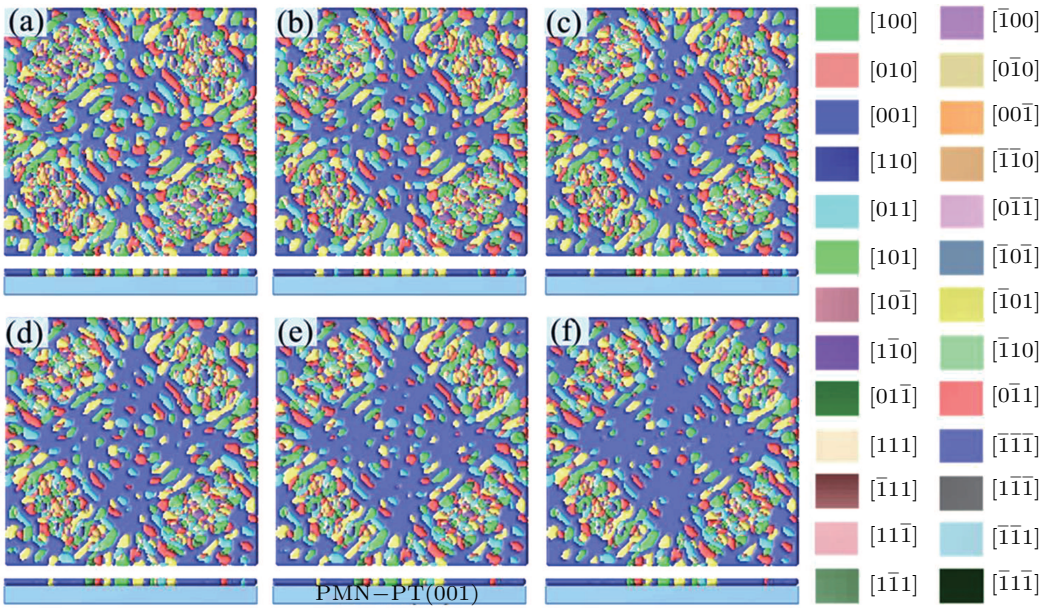


Fig. 3. (color online) Simulated magnetic domains structures of the $L1_0$ FePt (3 nm) thin film with the same reversible magnetic field H = 2.0 kOe but different compressive strains, (a) 0.00%, (b) −0.02%, (c) −0.03%, (d) −0.04%, (e) −0.05%, and (f) −0.06%, corresponding to the points *O*, *P*, *Q*, *R*, *S*, and *T* in Fig. 1(a).

Figure 4 shows the effect of compressive strain on the magnetic energy densities of the $L1_0$ FePt (3 nm) thin film at various reverse magnetic fields (20 kOe to −20 kOe). Figure 4(a) shows that the external magnetic field energies increase initially and then decrease with the external magnetic field decreasing from 20 kOe to −20 kOe, and the energy maximum appears at −2.206 kOe. Figures 4(b) and 4(c) show that the magnetic anisotropic energies and magnetic exchange energies are zero in the first place, and then gradually increase from zero to a maximum when the magnetic field decreases from 20 kOe to −3.0 kOe, which finally decrease to zero with the magnetic field decreasing from about −3.0 kOe to

−20 kOe. The reason is that the [001] axis is an easy magnetization direction in the $L1_0$ FePt thin film. When the magnetic fields are large, the magnetic anisotropic energies and magnetic exchange energies are lower for the energy minimization; when the magnetic fields decrease to the coercivities, the magnetic moment deviates from the easy magnetization direction and the magnetic exchange interaction between magnetic moments becomes large. Figure 4(d) shows that the demagnetization energies have the largest values when the magnetization is perpendicular to the plane of the $L1_0$ FePt thin film along the external magnetic field direction. They start to decrease when the magnetization deviates from the normal direction of the $L1_0$ FePt thin film and increase again as the magnetization inclines to align perpendicular to the plane of the $L1_0$ FePt thin film. Figure 4(e) displays that the magnetoelastic energy is zero when there is no compressive strain on the $L1_0$ FePt thin film under the switching of the magnetic field changing from 20 kOe to −20 kOe. However, when there are different compressive strains acting on the $L1_0$ FePt thin film, the magnetoelastic energies are constant at high external magnetic fields and the energies peak values appear at coercivities fields, because the magnetoelastic energy can induce a PMA. Thus the magnetoelastic energy is lower when the applied magnetic field is larger, and energies peak values show up as magnetic moments in the $L1_0$ FePt thin film deviate from the normal direction in the magnetization reversible processes. Moreover, differences of magnetic energies are negligible among different compressive strains, which range from 0 to −0.06%, except magnetoelastic energies. The magnetoelastic energy in the $L1_0$ FePt thin film increases by leaps with compressive strain strengthening due to the increase of compressive stress in the $L1_0$ FePt thin film, which is also ascribed to the fact that the magnetoelastic energy affects the magnetic anisotropy so that the distribution of the easy magnetization axis is changed. The total magnetic energies are shown in Fig. 4(f), which determine the reversible magnetization processes. Therefore, the magnetization even inclines to align perpendicular to the plane of the $L1_0$ FePt thin film and perpendicular anisotropy is improved when the compressive strain becomes large.

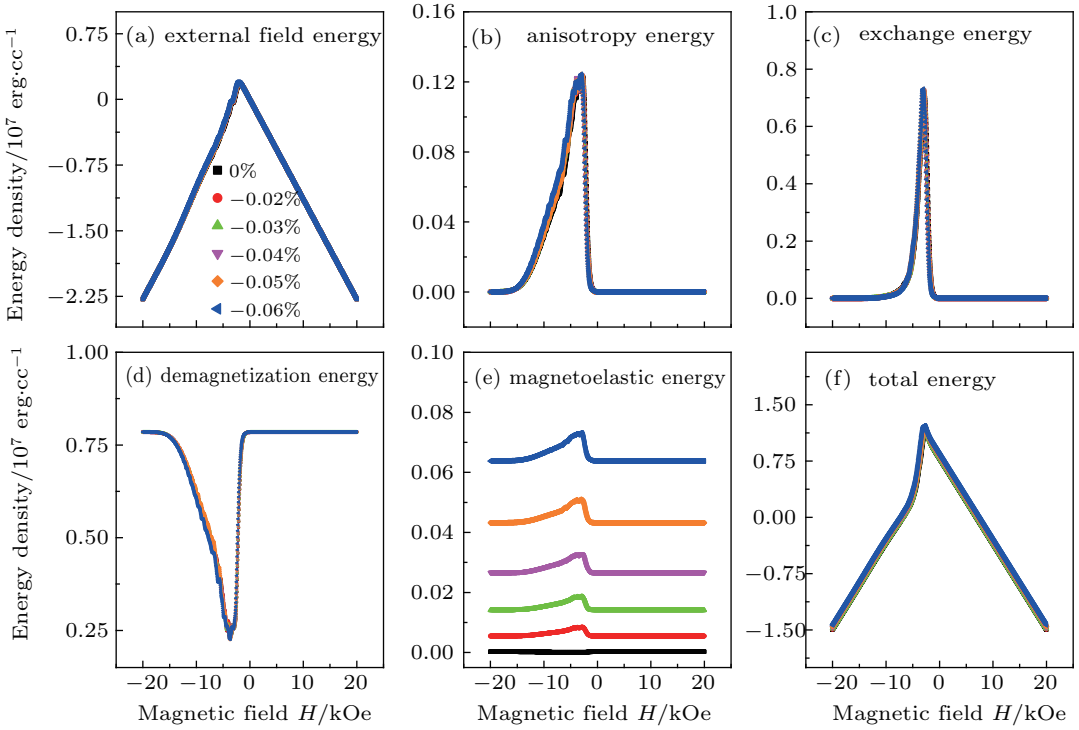


Fig. 4. (color online) Calculated magnetic energies densities of the $L1_0$ FePt (3 nm) thin film in magnetization reversible processes with different compressive strains. (a) External field energies, (b) anisotropy energies, (c) exchange energies, (d) demagnetization energies, (e) magnetoelastic energies, and (f) total energies.

4. Conclusion

We apply the three-dimensional phase field model to study the effect of compressive misfit strains on the magnetic properties and magnetization reversible processes of the $L1_0$ FePt (3 nm) thin film. Results show that the magnetic coercivities increase with the decrease of compressive strains from 0% to −0.06%, which agrees well with the experimental results.[23] The evolution of the magnetic domain structure of the $L1_0$ FePt thin film under a compressive strain −0.06 shows that the magnetization changes from [001] single domain to multidomain, and then to $[00\bar{1}]$ single magnetic domain at the reversible magnetization processes. The magnetization perpendicular to the $L1_0$ FePt thin film plane inclines to along the [001] direction and reverses tardily when the com-

pressive strain becomes larger. The calculated magnetic energy densities show that the main reason for the increase of coercivities as the compressive strain increases is the enhancement of magnetoelastic energy. When different compressive strains act on the $L1_0$ FePt thin film, the magnetoelastic energies are constant at a high external magnetic field and the energies peak values appear at the coercivities field, which is due to the fact that magnetoelastic energy induces the PMA, thus causing the magnetoelastic energy lower at the larger applied magnetic field. Meanwhile, when the magnetization deviates from the normal direction of the plane of the $L1_0$ FePt thin film, the energies peaks appear in the magnetization reversible processes.

Acknowledgment

The simulations were performed on the National Supercomputer Center in Guangzhou.

References

[1] Sepehri-Amin H, Iwama H, Ohkubo T, Shima T and Hono K 2017 *Scr. Mater.* **130** 247
[2] Wang J, Hata S, Takahashi Y K, Sepehri-Amin H, Varaprasad B S D Ch S, Shiroyama T, Schreflc T and Hono K 2015 *Acta Mater.* **91** 41
[3] Feng C, Zhao J C, Yang F, Hao S J, Gong K, Hu D, Cao Y, Jiang X M, Wang Z Q, Chen L, Li S R, Sun L, Cui L S and Yu G H 2016 *ACS Appl. Mater. Interfaces* **8** 7545
[4] Quarterman P, Wang H, Qiu J M, Guo H H, Ma B, Liu X Q and Wang J P 2015 *Appl. Phys. Lett.* **107** 232401
[5] Xu D B, Sun C J, Chen J S, Heald S M, Sanyal B, Rosenberg R A, Zhou T J and Chow G M 2015 *J. Phys. D: Appl. Phys.* **48** 255001
[6] Lupo P, Orna J, Casoli F, Nasi L, Ranzieri P, Calestani D, Algarabe P, Morellón L and Albertini F 2013 *EPJ. Web Conf.s* **40** 08001
[7] Moriyamaa T, Mitani S, Seki T, Shima T, Takanashi K and Sakuma A 2004 *J. Appl. Phys.* **95** 6789
[8] Feng C, Zhao J C, Yang F, Gong K, Hao S J, Cao Y, Hu C, Zhang J Y, Wang Z Q, Chen L, Li S R, Sun L, Cui L S and Yu G H 2016 *Sci. Rep. UK* **6** 23878
[9] Goyal R, Arora N, Kapoor A, Lamba S and Annapoorni S 2017 *J. Alloy. Compd.* **695** 1014
[10] Tao L, Liu D P, Liang S H, Han X F and Guo H 2014 *Euro Phys. Lett.* **105** 58003
[11] Ho P, Evans R F L, Chantrell R W, Han G C, Chow G M and Chen J S 2015 *J. Appl. Phys.* **117** 213901
[12] Tsai W C, Liao S C, Huang K F, Wang D S and Lai C H 2013 *Appl. Phys. Lett.* **103** 252405
[13] Lee M, Choi H and Chung Y C 2013 *J. Appl. Phys.* **113** 17C729
[14] Weller D, Mosendz O, Parker G, Pisana S and Santos T S 2013 *Phys. Status Solidi A* **210** 1245
[15] Zhang L R, Liu L W, Hayasaka K and Ishio S 2015 *J. Alloy. Compd.* **651** 389
[16] Barmak K, Kim J, Shell S, Svedberg E B and Howard J K 2002 *Appl. Phys. Lett.* **80** 4268
[17] Sun A C, Kuo P C, Chen S C, Chou C Y, Huang H L and Hsu J H 2004 *J. Appl. Phys.* **95** 7264
[18] Li Y L, Huang A P, Feng T F, Chen Q, Shu X L, Chen J Y, Chen Z Y 2011 *Chin. Phys. Lett.* **28** 067502
[19] Wang L Z, Miao J Y, Zhao Z, Liu C and Wei D 2017 *Chin. Phys. Lett.* **34** 027501
[20] Ho H, Zhu J X, Kulovits A, Laughlin E and Zhu J G 2014 *J. Appl. Phys.* **116** 193510
[21] Varaprasad B S D Ch S, Takahashi Y K, Wang J, Ina T, Nakamura T, Ueno W, Nitta K, Uruga T and Hono K 2014 *Appl. Phys. Lett.* **104** 222403
[22] Dong K F, Li H H and Chen J S 2013 *J. Appl. Phys.* **113** 233904
[23] Liu M F, Hao L, Jin T L, Cao J W, Bai J M, Wu D P, Wang Y and Wei F L 2015 *Appl. Phys. Express* **8** 063006
[24] Hu J M, Duan C G Nan C W and Chen L Q 2017 *NPJ Comput. Mater.* **3** 18
[25] Kazaryan A, Wang Y, Jin Y M, Wang Y U, Khachaturyan A G, Wang L S, David E and Laughlin 2002 *J. Appl. Phys.* **92** 7408
[26] Liu L W, Ohsasa K, Koyama T, Liang L Y, Zhang L R and Ishio S 2015 *IEEE Trans. Magn.* **51** 3201903
[27] Chen L Q 2002 *Annu. Rev. Mater. Res.* **32** 113
[28] Rao W F, Wuttig M and Khachaturyan A G 2011 *Phys. Rev. Lett.* **106** 105703
[29] Wang Y U, Jin Y M and Khachaturyan A G 2004 *Acta Mater.* **52** 81
[30] Liu L W, Zhang L R, Liang L Y, Ohsasa K, Koyama T, Sheng Q, Hasegawa T and Ishio S 2016 *J. Alloy. Compd.* **682** 176
[31] Rao W F and Khachaturyan A G 2012 *Acta Mater.* **60** 443
[32] Hu J M, Li Z, Chen L Q and Nan C W 2011 *Nat. Commun.* **22** 553
[33] Hu J M, Yang T N, Chen L Q and Nan C W 2013 *J. Appl. Phys.* **114** 164303
[34] Hu J M, Sheng G, Zhang J X, Nan C W and Chen L Q 2011 *Appl. Phys. Lett.* **98** 112505
[35] Hu C C, Yang T N, Huang H B, Hu J M, Wang J J, Shi Y G, Shi D N and Chen L Q 2016 *Appl. Phys. Lett.* **108** 141908
[36] Khachaturyan A G 1983 *Theory of Structural Transformations in Solids* (New York: Wiley)
[37] Li Y L, Hu S Y Liu Z K and Chen L Q 2002 *Acta Mater.* **50** 395